Transient analyses for a molten salt fast reactor with optimized core geometry

R. Li [a,*], S. Wang [a], A. Rineiski [a], D. Zhang [a], E. Merle-Lucotte [b]

[a] Institute for Nuclear and Energy Technologies (IKET), Karlsruhe Institute of Technology (KIT), Hermann-von-Helmholtz-Platz 1, D-76344 Eggenstein-Leopoldshafen, Germany
[b] Laboratoire de Physique Subatomique et de Cosmologie – IN2P3 – CNRS/Grenoble INP/UJF, 53, rue des Martyrs, 38026 Grenoble, France

HIGHLIGHTS

- MSFR core is analyzed by fully coupling neutronics and thermal-hydraulics codes.
- We investigated four types of transients intensively with the optimized core geometry.
- It demonstrates MSFR has a high safety potential.

ARTICLE INFO

ABSTRACT

Molten salt reactors (MSRs) have encountered a marked resurgence of interest over the past decades, highlighted by their inclusion as one of the six candidate reactors of the Generation IV advanced nuclear power systems. The present work is carried out in the framework of the European FP-7 project EVOL (Evaluation and Viability Of Liquid fuel fast reactor system). One of the project tasks is to report on safety analyses: calculations of reactor transients using various numerical codes for the molten salt fast reactor (MSFR) under different boundary conditions, assumptions, and for different selected scenarios. Based on the original reference core geometry, an optimized geometry was proposed by Rouch et al. (2014. Ann. Nucl. Energy 64, 449) on thermal-hydraulic design aspects to avoid a recirculation zone near the blanket which accumulates heat and very high temperature exceeding the salt boiling point. Using both fully neutronics thermal-hydraulic coupled codes (SIMMER and COUPLE), we also re-confirm the efforts step by step toward a core geometry without the recirculation zone in particular as concerns the modifications of the core geometrical shape. Different transients namely Unprotected Loss of Heat Sink (ULOHS), Unprotected Loss of Flow (ULOF), Unprotected Transient Over Power (UTOP), Fuel Salt Over Cooling (FSOC) are intensively investigated and discussed with the optimized core geometry. It is demonstrated that due to inherent negative feedbacks, an MSFR plant has a high safety potential.

© 2015 Elsevier B.V. All rights reserved.

1. Introduction

Molten salt reactors (MSRs) have achieved as marked resurgence of interest over the past decades, highlighted by their inclusion as one of the six candidate reactors of the Generation IV (Serp, 2014) advanced nuclear power systems with expected remarkable advantages in safety, economics, sustainability, and proliferation resistance. The Oak-Ridge National Laboratory Molten Salt Reactor Experiment and the Molten Salt Breeder Reactor project (Weinberg, 1970) started the early studies for MSRs in the US. An innovative concept called Molten Salt Fast Reactor (MSFR)

(Nuttin et al., 2005; Mathieu and Heuer, 2006; Mathieu et al., 2009; Forsberg et al., 2007) has been proposed in view of the deployment of a thorium based reactor. Since 2011, the EVOL (Evaluation and Viability Of Liquid fuel fast reactor system) project was carried out within the EURATOM 7th framework programme (Merle-Lucotte and Heuer, 2012; Merle-Lucotte et al., 2013; Brovchenko et al., 2012). Based on the peculiarity of using a liquid fuel, this MSFR concept is derived from the US molten salt reactors, a major potential change is a return to the mode of "two fluid design", in which separate salts are used for the liquid fissile $LiF–ThF_4–^{233}UF_4$ and fertile $LiF–ThF_4$. A benchmark reactor concept for this pre-conceptual MSFR design has been set up during the EVOL project. The reactor geometry, fuel compositions, structure materials, etc. are studied in detail, and in order to gain a more rigorous insight into the MSFR features and capabilities, the MSFR operational and safety behavior

* Corresponding author. Tel.: +49 721 608 22336; fax: +49 721 608 23824.
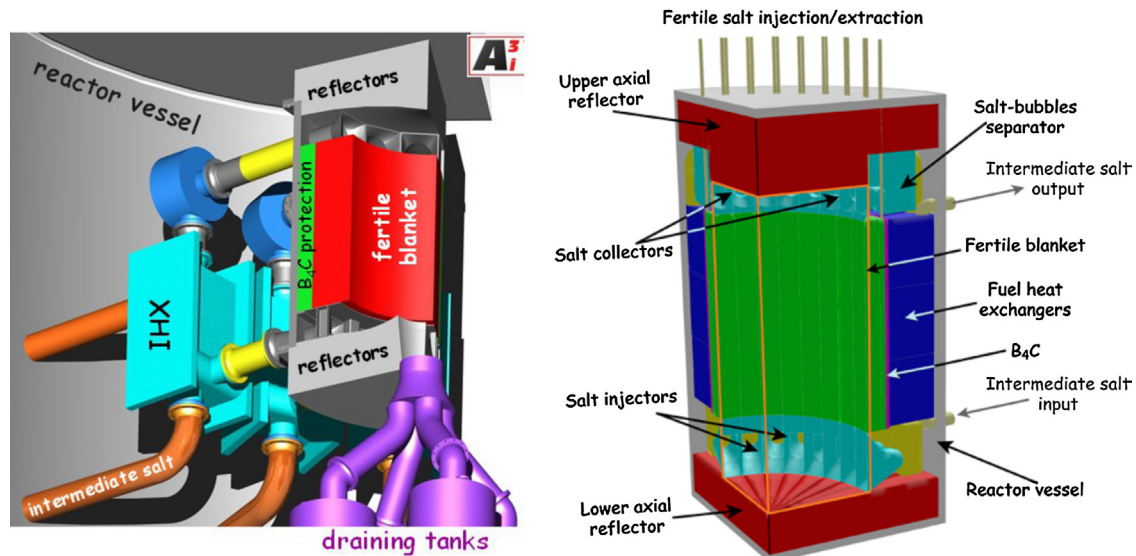E-mail address: rui.li@kit.edu (R. Li).

Fig. 1. (Left) Global view of a quarter of the reactor vessel including the fertile blanket (red), the B₄C protection (green), the structure in Ni-based alloy (gray), the heat exchangers (pale blue) and the draining tanks (purple); (right) schematic view of a quarter of the MSFR, the fuel salt (not represented here) being located within the orange lines (Brovchenko, 2013). (For interpretation of the references to color in this figure legend, the reader is referred to the web version of this article.)

have been explored with different numerical codes (Brovchenko et al., 2013b; Wang et al., 2014). The MSFR pre-conceptual design is shown in Fig. 1 (Brovchenko, 2013). The fuel salt flows upwards in the active core until it reaches an outlet area which leads to salt-bubble separators through salt collectors. The salt then flows downwards in the fuel salt heat exchangers and the pumps before finally re-entering the bottom of the core through injectors. The injection and extraction of the salt is performed through pipes of about 30 cm diameter.

In the calculation model the external circuit (salt collector, salt-bubble separator, heat exchanger, pump, salt injector and pipes) is subdivided into 16 identical modules distributed around the core, outside the fertile blanket and within the reactor vessel. The external circuit is divided into two parts: the pipes (including the salt-bubble separator, the pump and the injector) and the heat exchanger. The distribution of the salt between these two parts is chosen so as to minimize the pressure drops in the circuit. The fuel salt runs through the whole cycle in 3.9 s. The salt circulation being considered uniform, the residence time of the salt in each zone of the circuit and the core is proportional to the volume of this zone. The total fuel salt volume is distributed half (9 m³) in the core and half (9 m³) in the external circuit. The external core structures and the heat exchangers are protected by thick reflectors (1 m height for the axial reflectors) made of nickel-based alloys which have been designed to absorb more than 99% of the neutrons from the core region. The temperature range of the MSFR design, namely between salt freezing (838 K) and melting of the nickel alloy for the core structures (approximately 1600 K), need to be considered as the margin points when performing steady state and transients calculations (Fiorina et al., 2014).

Additional information about the recent MSFR safety analyses can be found in the open literature (Aufiero et al., 2014; Fiorina et al., 2014; Rouch et al., 2014). Basically our results are analogous to those described in the cited references, but we are using different codes independently. It is very important to do so, using different safety analysis codes applied for molten salt reactor transient behavior simulations, since the available experimental data is scarce and incomplete (Wang et al., 2014). In this paper we discuss mainly the optimized core geometry of the MSFR design and its analysis of certain transients because of the strong coupling between the thermal hydraulics and the neutronics (due to the

reactivity feedback coefficient). MSFR safety studies done with the SIMMER-III code (Wang et al., 2006) and the COUPLE code (Zhang and Rineiski, 2014) are described in this paper. SIMMER-III is a two-dimensional, multi-velocity field, multi-phase, multi-component, Eulerian fluid-dynamics code coupled with a structure model and a space-, time- and energy-dependent neutron dynamics model. It was originally developed for severe accident analyses of sodium cooled fast reactors. The SIMMER-III code as a versatile and flexible tool is applied to transient simulation and the safety analysis of various reactor types with different coolants and neutron spectra. This code was extended by KIT to be able to deal with molten salt reactors (Wang et al., 2006, 2013). To provide a fast calculation tool for MSR transient analyses near operating conditions, a neutronics and thermal hydraulics coupled code named COUPLE has been developed at KIT/IKET recently. The COUPLE code is initially developed for the neutronics and thermal hydraulics coupled calculation of liquid-fuel reactors including the molten salt reactors. COUPLE has been applied to MSFRs for its reference geometry to investigate steady state and transients calculations (Brovchenko et al., 2013a; Zhang et al., 2013; Zhang and Rineiski, 2014).

2. A hotspot free core geometry

2.1. MSFR reference core geometry

For the preliminary conceptual design, the thermal-hydraulic coupled neutronic simulation was carried out with the SIMMER-III code. The original MSFR core reference geometry with each marked component is shown in Fig. 2 (left) and its main parameters are listed in Table 1. According to the SIMMER-III simulation results as shown in Fig. 2 (right), it has been observed that a wide recirculation zone exists adjacent to the blanket. Additional investigation revealed that recirculation building up is due to inertial and viscous effects, as intentional omission of the gravity force in the calculation does not impact significantly these results. In the recirculation zone close to the blanket, the predicted temperature is very high forming a hotspot in the temperature distribution in Fig. 2 (right).

The wide recirculation zone exists in the core close to the blanket, in which the fuel is nearly stagnating in particular near the axial reflectors. Small secondary flow in the right down corner region can be also observed. The flow leaving the core in the top-right part is
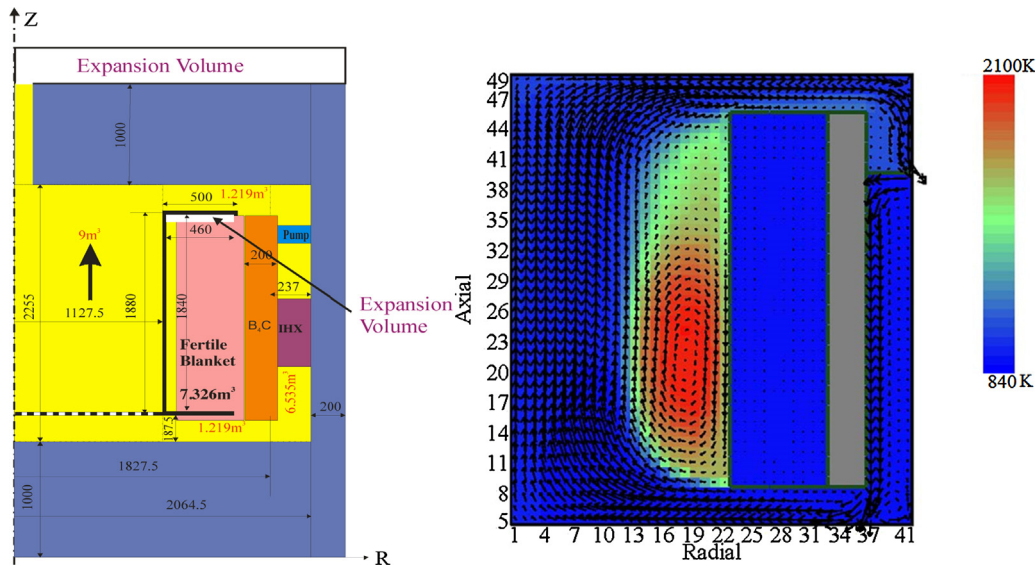
Fig. 2. (Left) Simplified MSFR configuration in 2D geometry, unit: mm; (right) Temperature distribution (K) with the hotspot, axial number is mesh numbering.

Table 1
Main parameters of MSFR under operational condition.

Parameter	Values
Thermal power (MW)	3000
Fuel molten salt initial composition	LiF–ThF$_4$–^{233}UF$_4$
Blanket molten salt initial composition	LiF–ThF$_4$
Input temperature (K)	923
Output temperature (K)	1023
Core dimensions (m)	R: 1.1275, H: 2.255
Fuel salt volume (m^3)	18
Typical velocity in the active core (m s^{-1})	2.8
Fuel circulation period in the system (s)	3.9

due to the pressure boundary condition as the pump is modeled in those meshes. The recirculation exceeding outlet temperatures leads to high temperatures inside the core region thus forming a hotspot region. In the recirculation zone close to the blanket, the predicted temperature is about several hundred degrees higher than the outlet temperature. In the recirculation zone close to the blanket, the hotspot also generates unnecessary thermal stress and material problems which should be avoided by a suitable thermal hydraulic design. Due to the recirculation problem, the maximum molten salt temperature reaches about 2100 K, the salt temperature reaches temporally its boiling point, not to mention that it already exceeds the MSFR temperature upper limit of 1600 K. As an advanced code including the phase change module, SIMMER code is not expected to obtain a steady state result due to such hotspot problem. The simulation ends with the salt vaporization. Therefore, the original reference geometry has to be changed. The highest temperature (2100 K) in the recirculation region by SIMMER is higher than obtained in Fiorina's work (i.e. Fig. 6, Fiorina et al., 2014), the coarse meshes and lack of turbulence models may be ascribed to the discrepancy. However, both investigations from Fiorina and us suggested the original reference geometry has to be optimized to avoid such a high temperature.

2.2. MSFR core geometry modifications

In order to improve the fluid flow pattern, Rouch et al. (2014) have proposed a hourglass shaped core with curved inlet and out let tubes and core wall. The optimized geometry was estimated and analyzed by a thermal-hydraulics code. As one of the prerequisites, a fully neutronics thermal-hydraulics calculation is needed. The optimization is re-confirmed by using the neutronics thermal-hydraulics code SIMMER. These activities are described in the following sub-sections.

2.2.1. Lower left corner of fertile blanket shape modified

As a first modification, the fertile blanket at the core inlet region is rounded instead of using an annular section torus, as shown in Fig. 3, which also shows the temperature distribution in this modified core. As compared to the original benchmark geometry with an annular section torus, the recirculation zone becomes smaller for the new blanket shape. However, a recirculation zone still exists. The maximum salt temperature in the center of nearly stagnant recirculating fuel decreases to around 1990 K (please note in each optimized step the maximal temperature legend varies in the figures). That is to indicate that only a limited improvement of the core thermo-hydraulic parameters has been achieved with this geometry modification. In Fig. 3 (right) the salt flow "suddenly" turns left in the lower part, the reason is that some orifice coefficients are added in the middle part of the external circuit to obtain the correct mass flow rate and pressure.

2.2.2. Upper left parts of fertile blanket shape modified

An additional fertile blanket modification was considered to round the part close to outlet zone. The fertile blanket now has a trapezoidal cross section shape instead of consisting of an annular section torus. It helps to mitigate the fuel salt hot spot issues, as shown in Fig. 4, which also gives the temperature distribution in this modified core. However, the recirculation zone still cannot be avoided completely. Compared to Fig. 3, the maximum salt temperature of the hotspot decreases only slightly, by a few degrees. During these simulations it was recognized that the recirculation is related to a high fluid velocity at the core inlet.

2.2.3. Inlet and outlet pipe shape modified

The piping system allows the circulation of the salt through the core, the heat exchanger and the pumps. The pipes are primarily sized (diameter and length) according to two main objectives: to reduce the fuel salt volume outside the core and to limit the maximum salt speed in the pipes (to avoid erosion). The salt's circulating time is assumed to be 3.9 s in the original preliminary conceptual design. Variations in the pipes diameter impact the circulation period of the fuel salt in the whole system, and, thus, its heating in
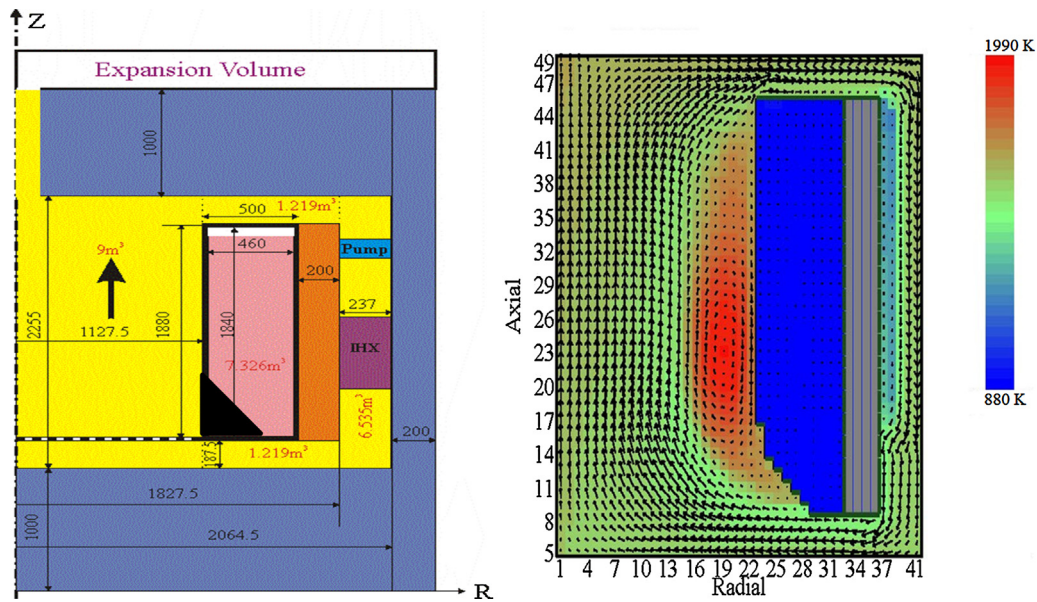
Fig. 3. Optimized geometry evolution (Step I): (left) lower left part of fertile blanket shape modified; (right) temperature distribution (K) with the hotspot.

the core if the power is fixed. A closer examination of the results of the simulation described in Sections 2.2.1 and 2.2.2 revealed that the molten salt velocity at the inlet and outlet pipes of the original preliminary conceptual design is probably too high to prevent appearance of the recirculation region and the hotspot in the core. To avoid this hotspot problem, one may modify the core inlet pipe shape to get a better flow mixture with the recirculation zone by adding an extra no-flow part in the lower-left region as indicated in Fig. 5. It can also be seen in Fig. 5 that the high temperature molten salt is pushed up to the upper-middle part of the core. The maximum molten salt temperature is about 1250 K, and location of the hot salt region is far from the blanket.

Accordingly the shape of the outlet pipe is modified as well. Finally Fig. 6 shows the 2D optimized geometry proposed by Rouch et al. (2014), the black part is steel. One may also find its corresponding 3D geometry in literature. It is a suitably modified core

geometry, in which the inlet and outlet pipe shapes are modified, the fertile blanket also reshaped to improve the molten salt flow pattern. With these modifications, the recirculation region and the hotspot near the blanket is eliminated. As so far, the safety margin is obviously improved by the proposed optimized core geometry.

3. COUPLE code and its modeling on the optimized geometry

3.1. Fluid dynamics modeling

It is clear that turbulence effects need to be considered since the fuel/coolant velocity is relatively high (for instance, the Reynolds number in around 4600 in the primary side of the heat exchanger), in particular concerning its influence on temperature in case of transients (Zhang et al., 2013; Fiorina et al., 2014). The transient
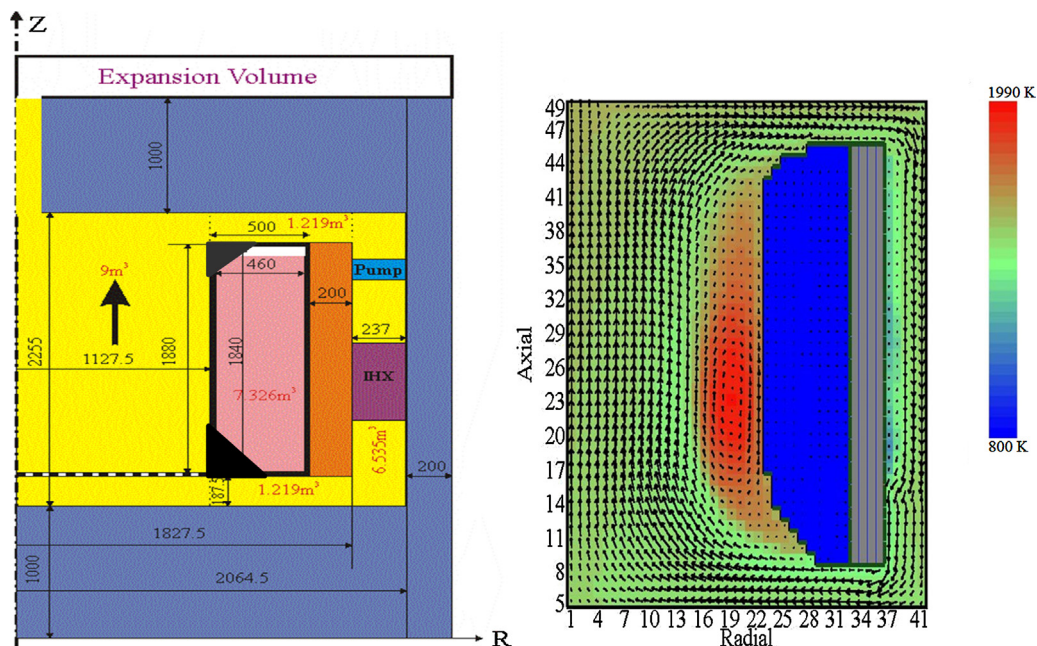

Fig. 4. Optimized geometry evolution (Step II): (left) upper left parts of fertile blanket shape modified; (right) temperature distribution (K) with the hotspot.
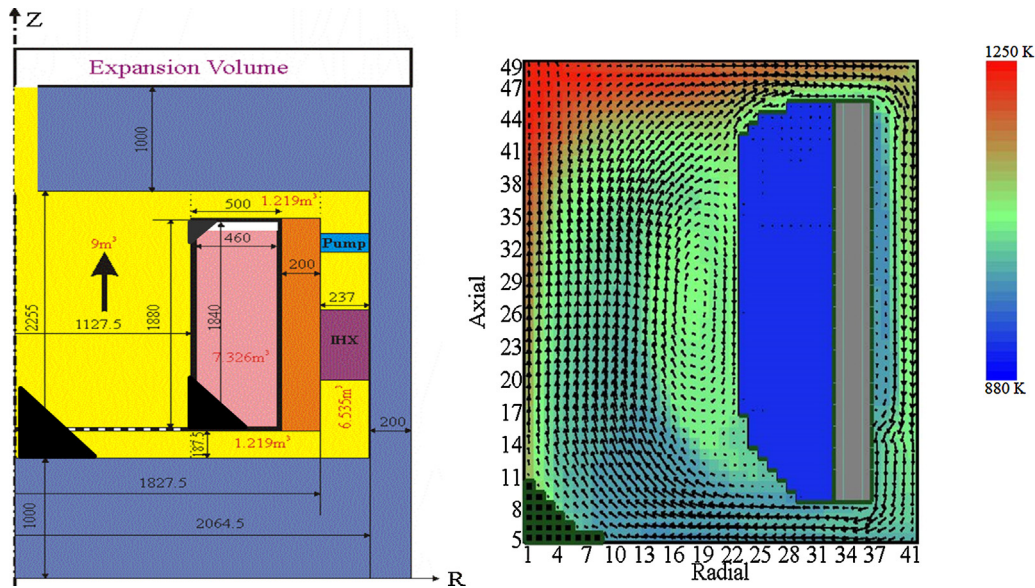
Fig. 5. Optimized geometry evolution (Step III): (left) Inlet pipe shapes modified; (right) temperature distribution (K) without the hotspot.
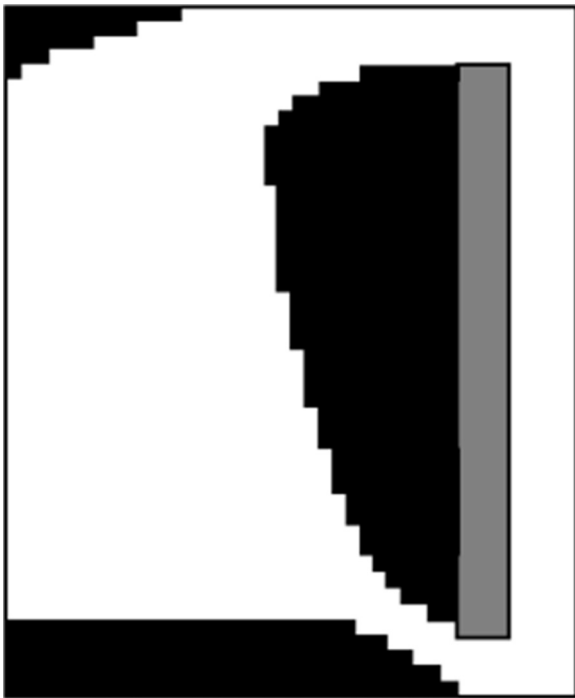

Fig. 6. Optimized geometry.

scenarios simulations are performed with the COUPLE code which includes a turbulence model as its particular merit for our analyses. The COUPLE code has been applied to the MSFR original reference design for steady state and transients simulation (Brovchenko et al., 2013a; Zhang and Rineiski, 2014). More information about the COUPLE code including the governing equations and its development have been presented in the previous publication (Zhang et al., 2013; Zhang and Rineiski, 2014). For simplicity here only some key points are addressed to allow a better understanding of the presented numerical results.

(1) Thermal expansion. The Reynolds Averaged Navier–Stokes (RANS) equations for mass, momentum and energy conservation are solved. The molten salt is considered as an incompressible liquid, but thermal expansion is modeled. The thermal expansion effect (the fissile mass inventory variation) is simulated by application of a suitable fuel thermal physical property model.

(2) Turbulence model. At the current stage of the MSFR design, some prospective studies (Aufiero et al., 2014; Rouch et al., 2014) have confirmed the accuracy of the results determined by using a k–ε model showing that it is appropriate for the MSFR application. The validation of the turbulence model of the COUPLE code has been performed with a single pipe flow benchmark case (Zhang and Rineiski, 2014). A suitable $y+$ is necessary to obtain accurate result when employing k–ε turbulence model and wall function. The $y+$ value for each volume element adjacent to the wall is kept less than 40 in our simulation. Another point is that compared with the original geometry, the flow pattern is influenced by the jigsaw boundary near the blanket. The mesh has passed the sensitivity analysis in particular concerning to the jigsaw shape.

(3) Pump model. The primary pumps driving force is modeled as body force in the momentum governing equation. The pump is assigned in the same manner as in SIMMER modeling, which is the right-middle part as indicated in Fig. 5. The natural convection also is modeled in the momentum equation via the gravity term. The local turbulent viscosity is obtained by solving the standard k–ε model with logarithmic wall functions.

(4) Intermediate heat exchanger model. It locates below the pump as indicated IHX in Fig. 5. It is modeled as a volume heat sink, it extracts simultaneously the power equal to the power produced in reactor core, and hence a time delay arises when the salt flows from core into the heat exchanger. As this simple model has limitations, it will be discussed in each transient.

3.2. Neutronics modeling

More focus is put for the neutronics modeling of the COUPLE code. As the salt flow effect on the delayed neutron precursor distributions in space is an inherent problem, it has been a big challenge in establishing the neutronics model for liquid-fuel reactors (Zhang et al., 2009, 2011).

(5) Diffusion theory. The multi-group diffusion theory is adopted. It consists of neutron diffusion equations for neutron fluxes,

Table 2
β_i and λ_i values for the delayed neutron precursors.

Family	β_i Delayed neutron fractions (pcm)	Decay constants λ_i (s^{-1})
1	10.9	1.31×10^{-2}
2	37.9	3.50×10^{-2}
3	45.3	1.27×10^{-1}
4	133.4	3.29×10^{-1}
5	50.3	9.1×10^{-1}
6	24.4	2.82×10^{0}

and balance equations for delayed neutron precursors. The essential difference compared with solid-fuel reactors, is the salt flow effect on neutron distribution.

(6) Salt flow effects. The salt flow effects are considered via additional convective terms in the neutron diffusion equations and neutron precursors balance equations, respectively.

(7) Two neutrons groups. The neutron energy range is subdivided into two groups: a fast neutron group and a thermal neutron group. The cross-sections are derived for each material using the TRAIN code (Rineiski, 2008) and JEFF-3.1 library.

(8) Six precursors families. Six families of precursors were generated by TRAINS code based on JEFF3.1 nuclear data libraries (JEFF3.1 itself provides eight families of precursors). Although a treatment with eight groups might be more accurate and suitable, six groups are considered sufficient for our current goal, namely to analyze MSFR kinetics. Furthermore six groups is the standard option in the SIMMER-III code. Moreover, the deviation caused by the difference of using eight instead of six groups is most probably only minor compare to the influences of still existing design uncertainties associated to the external part of the fuel circuit e.g. concerning details of the salt heat exchangers and the correlated uncertainties of the ex-core fuel residence time which is essentially influenced by the assumed fraction of the external circuit volume as compared to the core volume. The fraction of delayed neutrons that are generated in an energy group is calculated and directly used in the multi-physics model as a source term for the corresponding precursor equations. The macroscopic cross-sections and data for delayed neutron fractions β_i and the decay constant λ_i of the i ($i = 1$–6) family precursor are listed in Table 2.

(9) Cross-sections interpolation. Cross-sections are assumed to be directly proportional to the local density, and cross-sections are interpolated for the local temperature on the basis of a pre-calculated table for 600 K; 900 K, 1200 K, 1500 K and 2100 K. The neutron fluxes are determined according to a multi-group diffusion approach explicitly adapted for taking into account delayed neutron precursors movement.

(10) Libraries sensitivity. Regarding the application of the JEFF-3.1 library the suitability of other modern nuclear data libraries has been investigated by Brovchenko (2013). Even if e.g. using ENDF/B-VII might be considered more appropriate, e.g. regarding the capture cross section U-233. The impact on the main results of our study would not be very pronounced for two reasons (a) we are not considering the fuel burnup, so that the concentration of U-234 is not important here. (b) Any deviation in the precise determination of the criticality induced by not using the best nuclear data currently available can easily be compensated by suitably changing the fraction of $^{233}UF_4/ThF_4$.

(11) Decay heat production is modeled as shown in Fig. 7 from burnup calculations using the TRAIN code. The decay ratio is set as 0.037 which indicates that 96.3% of heat source of the reactor core coms from fission heat and 3.7% from decay heat. The decay heat model has been applied to all transients except UTOP.
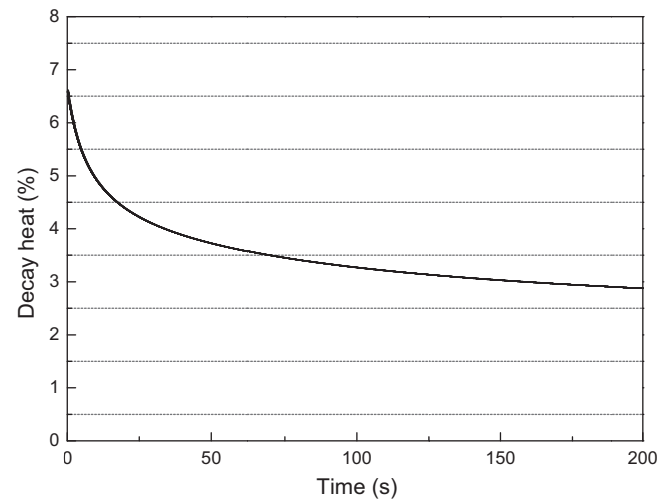

Fig. 7. Decay heat as a function of time after long operation.

3.3. Steady state simulation

The model using the COUPLE code has been set up for the optimized geometry. The mesh has passed the sensitivity analysis. Steady state conditions have been obtained. For simplicity only the temperature and power density distribution are displayed in R–Z geometry in Fig. 8, respectively. It can be also confirmed by COUPLE calculations that the location of the hotspot could be shifted. As a consequence of the flow pattern modification, the power density shape changes from a perfect sphere (in case of a perfectly spherical geometry) to a somewhat elliptical shape. The distributions of the concentration of the delayed neutron precursors of the six families are shown in Fig. 9, respectively. As delayed neutrons are moving through and moving out of the core, the delayed neutron source is a unique feature of the MSFR. It is noted due to the salt moving through and out of the core: the effective delayed neutron fraction is considerably reduced. One consequence is that, a higher fraction of prompt neutrons is needed in the core to keep the criticality. In our steady state calculation the β_{eff} is reduced to 137 pcm from 302 pcm for static fuel. It can be found that the distributions of the delayed neutron precursors are significantly influenced by the effect of salt recirculation. The delayed neutron precursors at the core center region have been shifted upper to the outlet of the reactor core. The fuel salt flow influences the precursors with smaller decay constants (long life) more strongly than those with larger decay constants (short life).

The power density and temperature shapes along the axial height at core center are shown in Fig. 10. Please note the sharp increase and decrease on the boundaries are due to the coarse mesh sizes used in the discretization. Our calculations shows the Doppler reactivity feedback coefficient (-4.31 dk/dT) which is comparable with the thermal expansion reactivity feedback coefficient (-3.93 dk/dT). The influence during a transient would be a combined process due to both effects from Doppler and thermal expansion. Hence it is recommended to use a combined "negative temperature reactivity feedback" for an interpretation with the transient phenomena, instead of indicating them separately.

It must be stated here that the performed analyses do not go deeply into the domain of severe accident scenarios (for instance, 2D geometry is a fairly major assumption). They do, however, determine which initiators and further additional failures could lead to severe accident conditions and whether there is a grace time available to perform corrective actions by e.g. an operator, i.e. whether an accident prevention and management strategy is feasible.
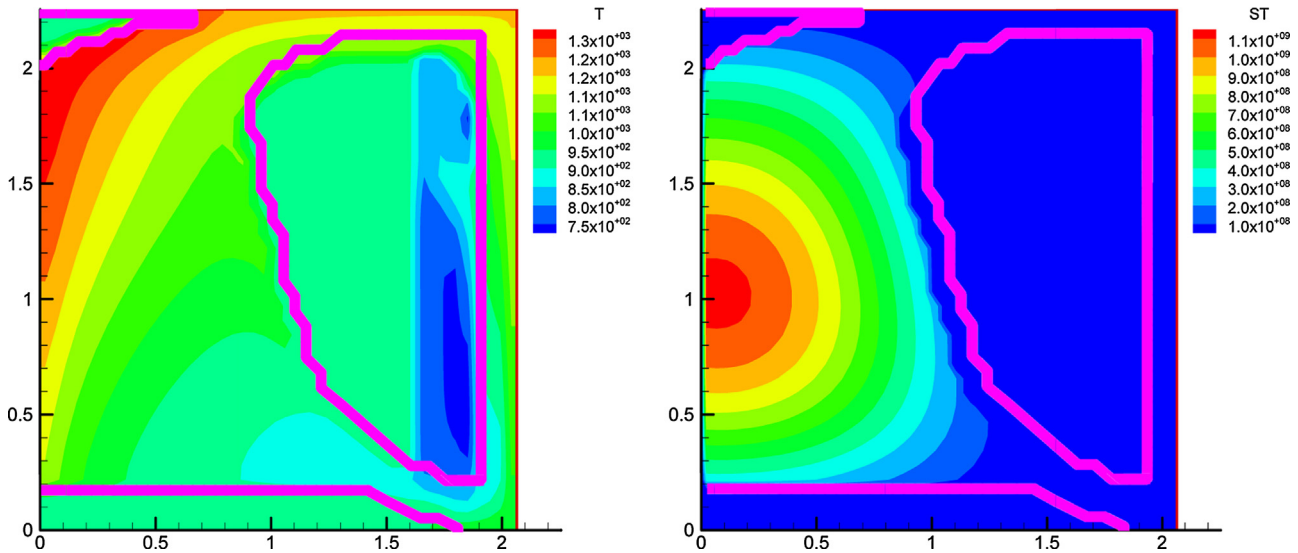
Fig. 8. Temperature (left, K) and power density (right, W m^{-3}) distribution of the optimized geometry.

4. Transient calculations for the optimized geometry

4.1. Unprotected Loss of Heat Sink (ULOHS)

A typical plant transient initiator that may be encountered during the operation of an MSFR is an Unprotected Loss of Heat Sink accident (ULOHS) or loss of cooling capabilities of the heat exchangers, which can generally be assumed as a loss of flow at the intermediate circuit (or a failure of the pump in the intermediate loop). The loss of cooling capabilities of the heat exchangers can be assumed to follow an exponential/or linear trend with an associated time constant or to happen promptly. During this transient scenario, the primary pump can be assumed to be operational.

ULOHS-1 assumes that power extracted by the heat exchanger decreases from 100% following an exponential trend with a time constant of 1 s. As soon as the cooling capabilities are lost, the core temperature rises, negative temperature reactivity feedback ensures that the power decreases quickly. It can be seen in Fig. 11 that a very fast core power decrease occurs at the very beginning of transient from $t = 0$ s to $t = 5$ s. From $t = 5$ s to $t = 50$ s the power finally slowly stabilizes at the decay heat level. After about 40 s the power doesn't change substantially, the decay heat is the only remaining power source. From $t = 5$ s to $t = 20$ s, the core outlet temperature reveals oscillations with slowly decreasing amplitude. The reason of oscillations (the average core temperature oscillates slightly as well) could be the direct mixture effort of the cooled and heated salt in the core region, due to our limitation on heat exchanger modeling. At the beginning the core outlet temperature decrease also quickly, then averaged core outlet temperature reveals an oscillation, this is because the hot and cold salt flows into and out of the core, alternately. After 20 s it substantially doesn't oscillate any more, since the generated power and the extracted heat are residing in another equilibrium state. The core outlet temperature keeps slightly increasing due to the decay heat, and the core outlet temperature reaches around 1150 K at $t = 50$ s.

ULOHS-2 assumes that power extracted by heat exchanger decreases from 100% to 50% following an exponential trend with time constant of 1 s. The smaller amount of heat extracted by the heat exchanger leads to a fictive introduction of a negative reactivity. As soon as the cooling capabilities are lost, the negative temperature reactivity feedback quickly reduces the reactor power. The outlet temperature increase clearly evident in Fig. 12 initially at $t = 5$ s is caused by the residual not immediately removed power by

the heat exchanger and decay heat. The core average temperature reaches a peak as the power reaches the bottom at $t = 7$ s. After the rapid temperature rise within the first 10 s, the temperature finally stabilizes at around 30 degrees higher than normal operation core outlet temperature. The decay heat is also included when the transient begins. The power decreases with a few oscillations until it stabilizes around half nominal power due to the coolant negative reactivity feedback.

For the sake of completeness, it should be mentioned that the intermediate circuit has been simulated in COUPLE as a heat exchanger namely IHX in Fig. 5. It is directly applied in the energy balance equation as a negative source term, depending neither on the temperature difference between primary and secondary circuits, nor on the heat transfer coefficients on each side of the heat exchanger. Under these assumptions the core inlet temperature varies only as a function of time of the extracted heat in the heat exchanger during the ULOHS. The temperature oscillations in ULOHS-1 are one of the consequences.

4.2. Unprotected Loss of Flow (ULOF)

The Unprotected Loss of Flow transient is analyzed via a primary pump coast-down function. It was assumed to be tripped with a time constant of 5 s at $t = 0$ s, the pump coast-down function is according to the following formula:

$$p = p_0 \left[\frac{1}{\left(1 + t/0.005 \right)} \right]$$

Fig. 13 (left) shows the primary pumps coast-down curve. The heat removal capabilities of the heat exchanger as modeled depends only on the primary molten salt flow rate, and not on the temperature difference between primary and secondary salt temperatures.

Fig. 13 (right) shows the heat exchanger normalized heat transfer capabilities' curve which is assumed as Dittus–Boelter equation:

$$Q = Q_0 \left[\frac{1}{\left(1 + t/0.005 \right)^{0.8}} \right]$$

Please note in our simulation the simulated ULOF is in fact a combined ULOF and ULOHS as the heat exchanger extracted power
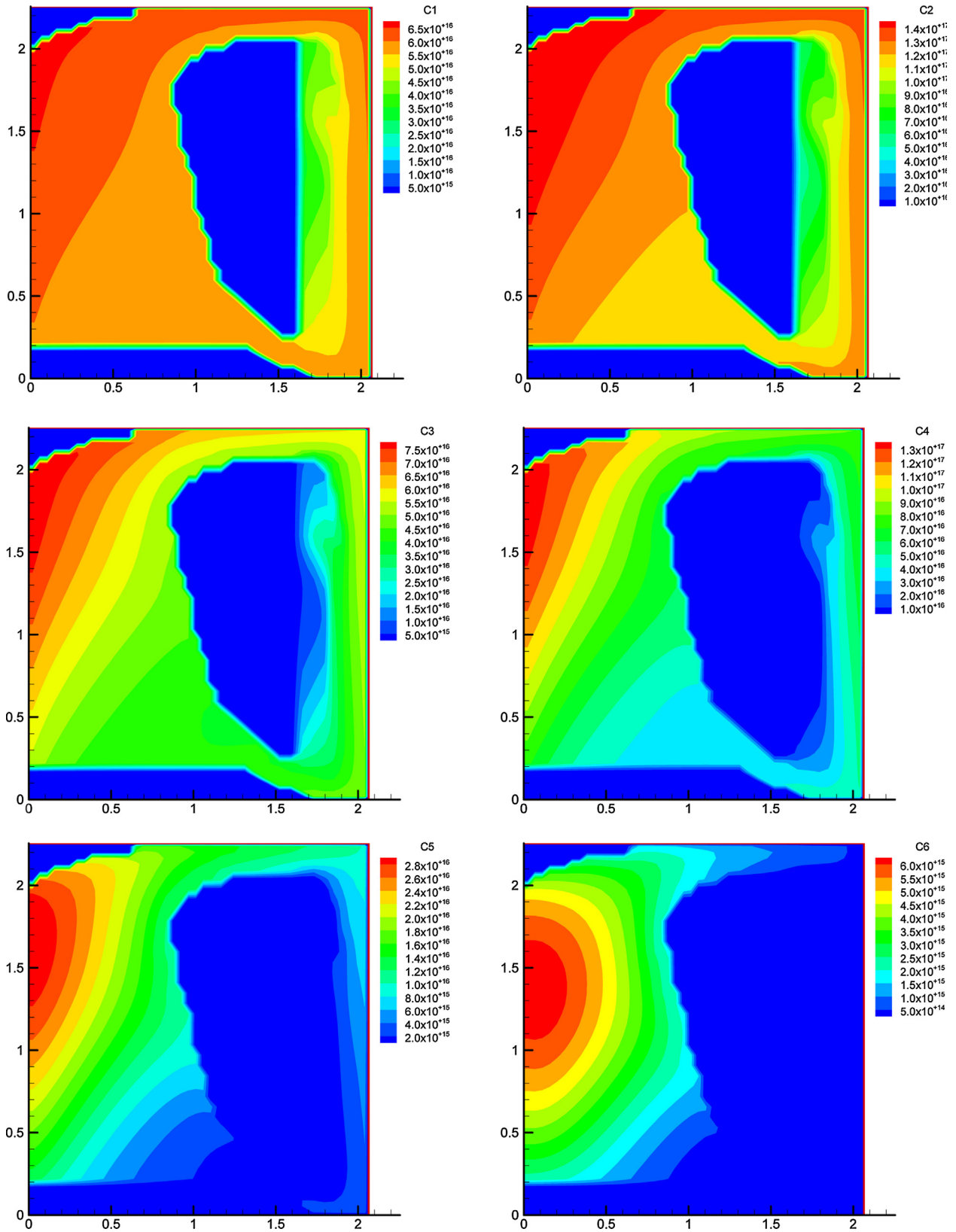
Fig. 9. C1–C6 (m^{-3} s^{-1}): the delayed neutron precursors (six families) distribution.

goes to zero. The condition of thermal insulation is applied at the external boundaries of the calculation geometry. Concerning heat transfer, the fluid and solid coupling model between salt and blanket structure wall, as well as between salt and reactor structures, is established by setting the heat conductive coefficients of the fluid and the solid.

Fig. 14 shows the evolution of the normalized power and core outlet temperature as function of time during ULOF. Please note the
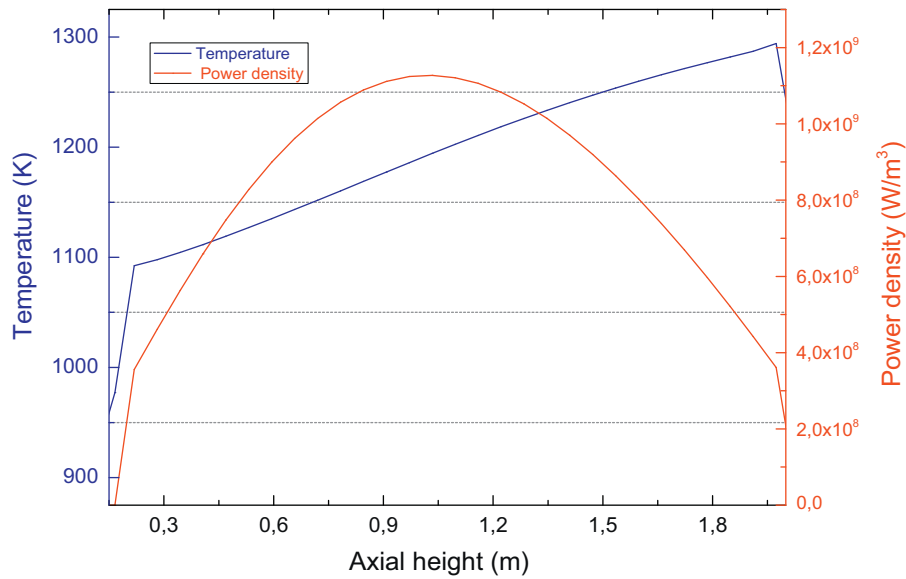
Fig. 10. The power density and temperature shape along axial height at core center.

starting point for P/P_0 on the y axis has not been chosen to be zero otherwise it would be difficult to distinguish the curve and x axis, the same comment also applies to Fig. 15. The k_{eff} falls below unit value very quick (0.7 s) after initiating the transient. During the first 20 s after the pump coast-down the power decreases quickly to the asymptotic power because of the negative temperature reactivity feedback. The core outlet temperature increases to around 1250 K, since the modeled heat removal capabilities of the heat exchangers depends on the primary molten salt flow rate. The increase rate of the core outlet temperature reveals the temperature feedback is fairly small. At the end of the calculation at 100 s the reactor power reduces to the asymptotic power level, as the heat exchangers still extract heat, until the decay heat remains as the only power source, a new steady state flow will be reached due to buoyancy effects. As the flow rate decreases, the fuel salt in the core has more time to be heated up, which results in a high core outlet temperature at $t = 100$ s as $T_{outlet} = 1250$ K. The results show that power decreases within 20 s from full power to the asymptotic level. However, the

core coolant outlet temperature increases by about 275 K at the end of the stabilization, and will continuously increase due to the decay heat if the reactor operator doesn't take actions properly. In the worst case, if freezing occurs in the heat exchanger due to the low salt flow rate after long time, the salt with high temperature will possibly melt the hot leg pipes. Therefore, such a possible melting scenario caused by salt freezing should be well taken care of in the future.

It has to be mentioned due to the numerical problem, a relatively small power growth in the initial phase (the first 2 s) takes place in case of ULOHS and ULOF. Such unphysical behavior is relevant to the heat exchanger modeling with the strong assumption of the same heat extraction from core, i.e. it takes around 2 s (the time needed for the salt moving from the heat exchanger to core) to response in the core in the case of the related transient of heat exchanger. During the 2 s, a small numerical decreased temperature results in a small power growth which is not physical.
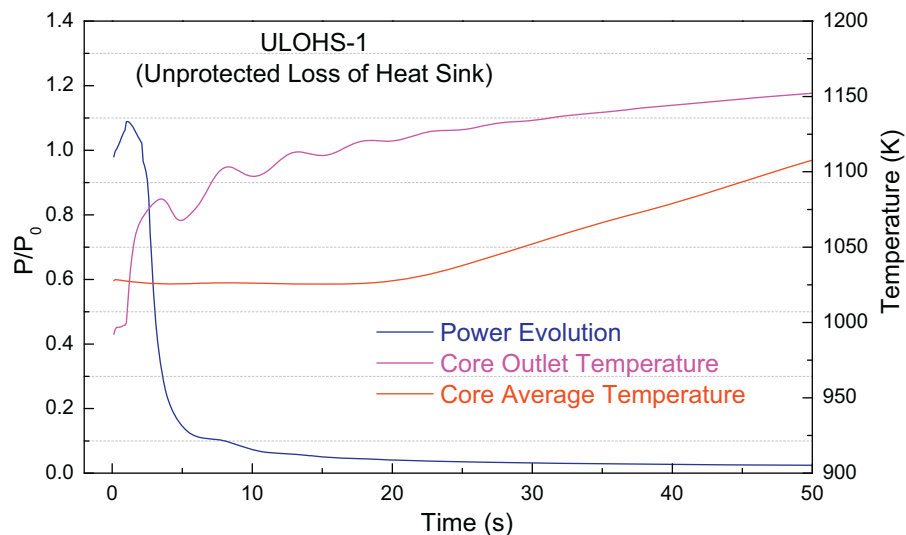

Fig. 11. Normalized power and core outlet/average temperature as function of time during ULOHS by an exponentially extracted power from 100% with a time constant of 1 s for the optimized core configuration.
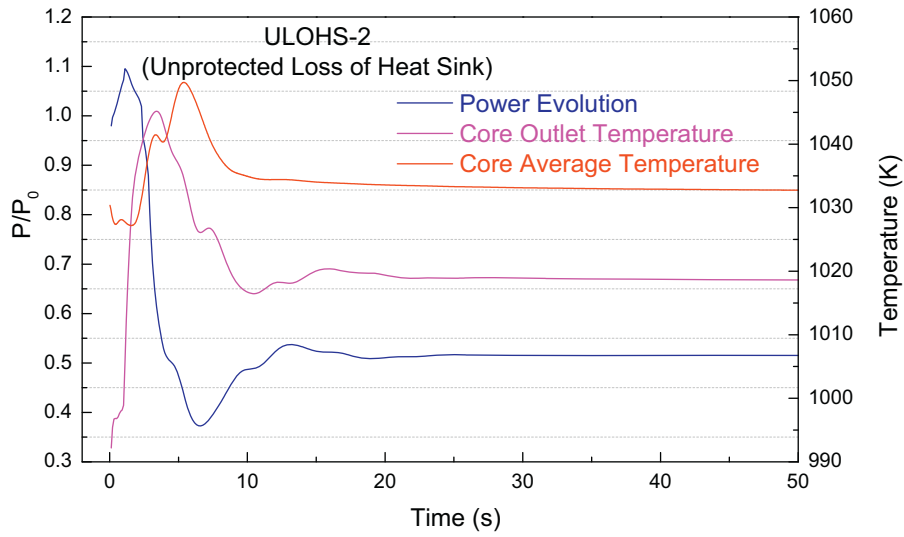
Fig. 12. Normalized power and core outlet/average temperature as function of time during ULOHS by an exponentially extracted power from 100% to 50% with a time constant of 1 s for the optimized core configuration.
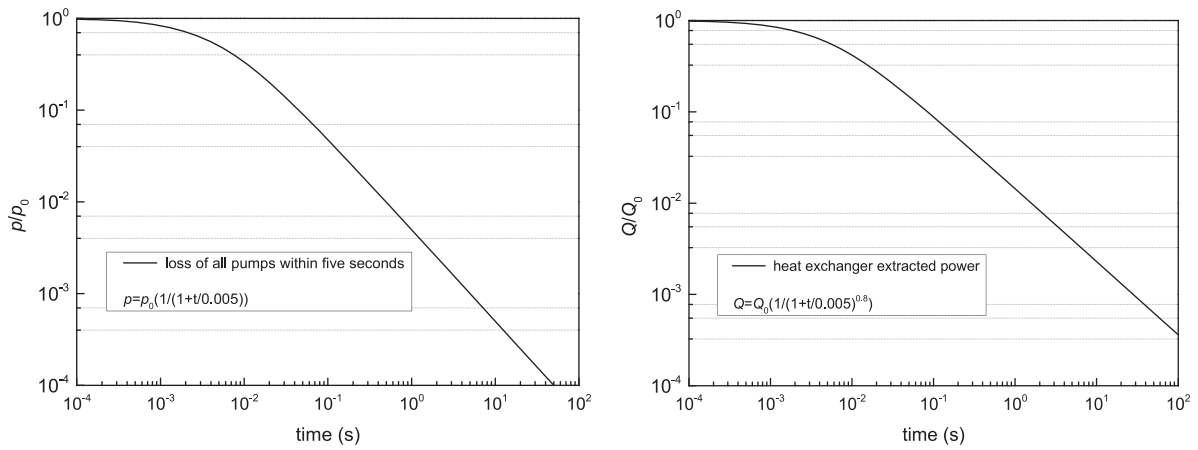

Fig. 13. (Left) The pumps coast-down function decreasing with a time constant of 5 s; (right) the heat transfer capabilities of the heat exchanger accompanied by pumps coast-down.
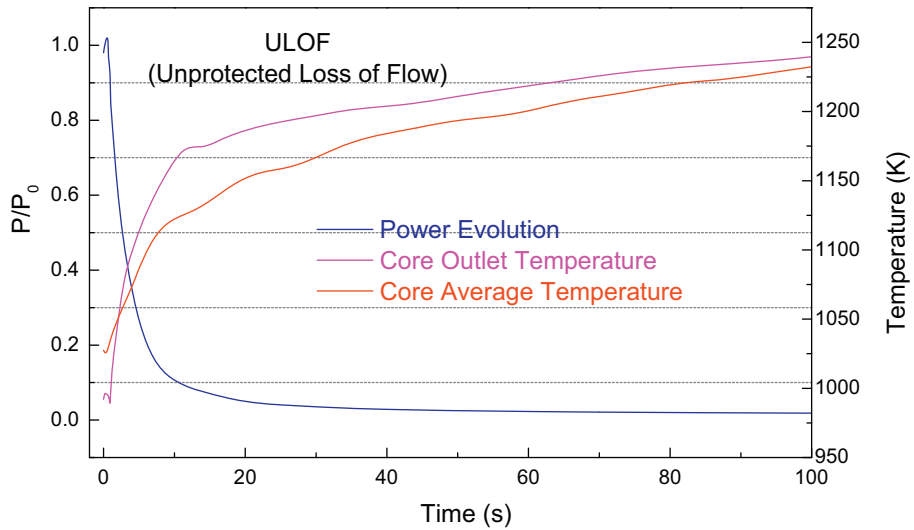

Fig. 14. Normalized power and core outlet/average temperature as function of time during ULOF for the optimized core configuration.
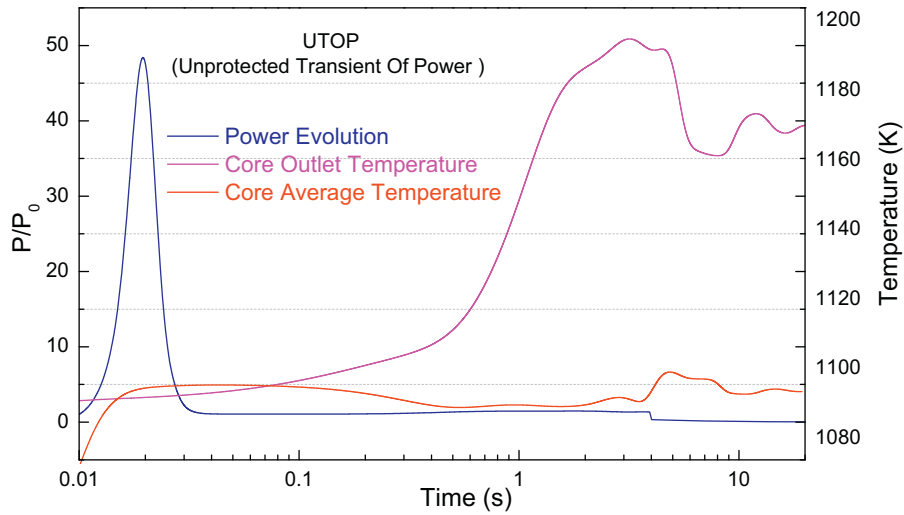
Fig. 15. Normalized power and core outlet/average temperature as function of time during UTOP for the optimized core configuration.

4.3. Unprotected Transient Over Power (UTOP)

A 300 pcm step-wise reactivity insertion is assumed as UTOP transient. COUPLE code in current version doesn't allow to impose a direct reactivity insertion e.g. a ramp rate stating from a steady state. In order to do a UTOP simulation, we modified artificially the cross sections to adjust it as if the k_{eff} has 300 pcm influences. As a result, the reactivity decrement is bigger i.e. the reactivity is lower compared with the results from Aufiero et al. (2014) and Fiorina et al. (2014). Fig. 15 shows the normalized power and core outlet temperature as function of time. As this figure shows, the total power excursion attains almost 50 times nominal power. After $t \approx 0.5$ s the reactivity insertion starts to remarkably increase the power, therefore the core outlet temperature becomes higher. Due to the negative temperature reactivity feedback, the increased temperature of the fuel salt leads to a decrease in reactivity. It leads temporarily to a normalized power, which roughly equals the initial steady state production rate. The introduction of reactivity will be compensated by the feedback of an increased temperature after some time. The core outlet temperature is $T \approx 1170$ K at $t = 20$ s, i.e. to a temperature increase of around 200 K compared to the

nominal condition. The extracted heat power by heat exchanger model simultaneously equals the power in the core during the simulation; therewith there is a delay effect when the salt flows from core into the heat exchanger.

4.4. Fuel Salt Over Cooling (FSOC)

In the scenario of Fuel Salt Over Cooling it is assumed that the extracted power capability is enhanced by 1.5 times. As a result of higher extracted heat capability, the core inlet temperature decreases when the cooled salt re-enters the active core region. As a consequence the power increases by roughly 1.7 times compared with the nominal power. As a consequence of the increasing power the core outlet temperature increases as shown in Fig. 16. When the high temperature salt re-enters into the active core region, the power decreases due to the negative temperature reactivity feedback. The power and core outlet temperature oscillations between 5 s and 30 s are induced by the salt circulation with different temperatures in alternate cycles. After damping of these oscillations the core outlet temperature increases until it stabilizes around 45 degrees higher than for nominal power operation. The power also
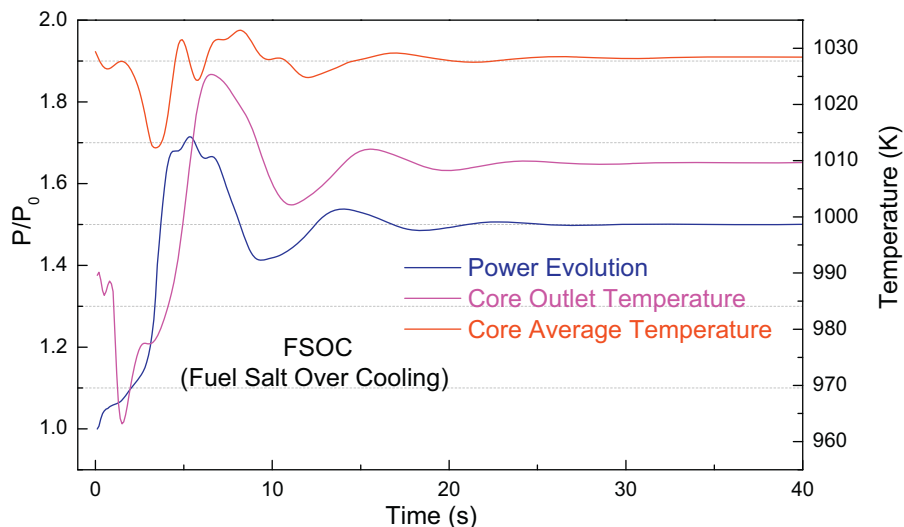

Fig. 16. Normalized power and core outlet/average temperature as function of time during FSOC for the optimized core configuration.
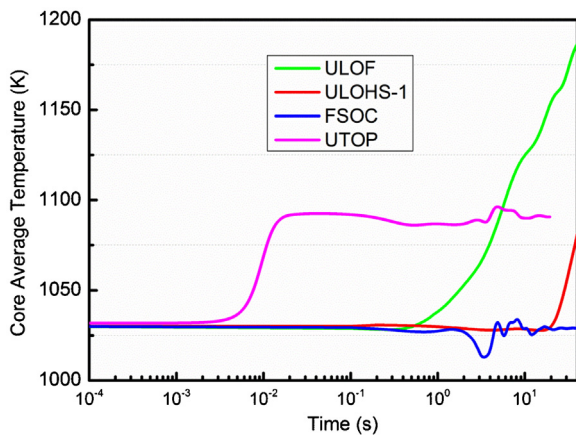
Fig. 17. Core average temperatures as function of time during all transients for the optimized core configuration.
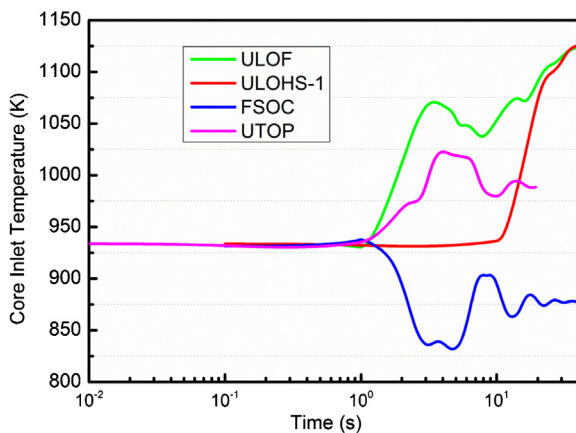

Fig. 18. Core inlet temperatures as function of time during all transients for the optimized core configuration.

reaches an asymptotic value corresponding to 1.5 times nominal power.

It takes around 4 s as a full recirculation period, i.e. every 4 s the over-cooled salt re-enter the core in the FSOC transient. That is to indicate the negative feedback receives a threshold input in every 4 s to decrease or increase the power. The fission power and core outlet temperature oscillations (with a period of 8 s as a full circle of decreasing and increasing) backtrack to the salt circulation with different temperature alternately, until the final core outlet temperature reaches an asymptotic value.

4.5. Other remarks

The sensors may be put in the core outlet to measure the temperatures, the core outlet temperatures are discussed in the previous sections. However, it is still interesting to check the average core since this core averaged temperature is the one more directly related to feedbacks as already shown in each chart. Here the comparisons of each transient are overviewed. The core averaged temperatures until 40 s (for ULOF 20 s due to the tiny time step) are shown in Fig. 17. For the transients ULOHS, ULOF and UTOP, the core averaged temperatures are higher than the steady state, while for FSOC transient the core averaged temperature stays the same as in steady sate after several oscillations. One can also observe the different negative feedback effects during different transients.

The core inlet (i.e. heat exchanger outlet) temperatures of four transients (for ULOHS, the first one ULOHS-1 is taken) are compared

Table 3
Summary of transients power characteristics and maximum core outlet temperatures.

Transient name	Power excursion peak (normalized)	Power stabilized time (s)	Maximal core outlet temperature (K)
Unprotected Loss of Heat Sink-1	1.1	25	1150
Unprotected Loss of Heat Sink-2	1.1	15	1045
Unprotected Loss of Flow	1.0	40	1250
Unprotected Transient Over Power	48	0.1	1187
Fuel Salt Over Cooling	1.8	20	1010

in Fig. 18, to study whether the salt freezing risk would occur among them. As it is clearly seen, the salt freezing possibility is not high except FSOC. The possible salt freezing may happen after 3 s following the transient FSOC, since the salt temperature reaches the freezing point (838 K). Therefore, despite the strong assumption of the heat exchanger model which is a rather conservative one, the further MSFR design should be including some mitigating effects to avoid such freezing risk. On the other hand, for code developing the phase change model should be included as well in the near future work.

5. Summary and conclusions

The purpose of the described analyses is to demonstrate the feasibility and safety of the reference MSFR design. For the reference MSFR active core, the liquid fuel builds up a recirculation region. In this recirculation region the salt flow is almost stagnant, causing excessive temperatures. The core with optimized geometry successfully overcomes the hotspot issue and the safety margin is obviously improved. The transient analyses could be summarized as follows:

Thanks to the negative temperature reactivity feedback coefficient including Doppler effects and thermal expansion, (1) The power stabilizes to decay heat level when the loss of cooling capabilities of the heat exchangers occurs, (2) after a pump coast-down, the power decreases quickly to the asymptotic power level, (3) for the overpower accidents, after a 300 pcm step-wise reactivity insertion, the current analysis demonstrates that this reactor can well be resistant to an overpower accident and (4) a over cooling transient can be stabilized after 20 s, nevertheless the risk of salt freezing should be overcome in the further design. The power excursion values and outlet maximum temperature during each transient are listed in Table 3, to summarize the results in a concise way.

The results of the different transient analyses demonstrate the MSFR's high safety potential. Further development of calculation models, accumulation of safety-relevant experimental results, design optimizations and additional safety analyses, in particular for hypothetical severe accidents, could provide an even more detailed understanding of MSFR safety issues.

References

Aufiero, M., Cammi, A., Geoffroy, O., Losa, M., Luzzi, L., Ricotti, M.E., Rouch, H., 2014. Development of an OpenFOAM model for the molten salt fast reactor transient analysis. Chem. Eng. Sci. 111, 390–401.

Brovchenko, M., Heuer, D., Merle-Lucotte, E., 2012. Preliminary safety calculations to improve the design of the molten salt fast reactor. In: Proceedings of PHYSOR 2012, Knoxville, USA.

Brovchenko, M., Merle-Lucotte, E., Heuer, D., Rineiski, A., 2013a. Molten salt fast reactor transient analyses with the COUPLE code. In: Proceedings of ANS Annual Meeting 2013, Atlanta, USA.

Brovchenko, M., Merle-Lucotte, E., et al., 2013b. Optimization of the pre-conceptual design of the MSFR—EVOL project. Deliverable D2, 2.

Brovchenko, M., 2013. Etudes préliminaires de sûreté du réacteur à sels fondus MSFR. Grenoble Institute of Technology (Ph.D. Thesis).

Fiorina, C., Lathouwers, D., Aufiero, M., Cammi, A., Guerrieri, C., 2014. Modeling and analysis of the MSFR transient behaviour. Ann. Nucl. Energy 64, 485–498.

Forsberg, C.W., et al., 2007. Liquid salt applications and molten salt reactors. In: Revue Générale du Nucléaire No 4/2007., pp. 63.

Mathieu, L., Heuer, D., 2006. The thorium molten salt reactor: moving on from the MSBR. Prog. Nucl. Eng. 48, 664–679.

Mathieu, L., Heuer, D., Merle-Lucotte, E., 2009. Possible configurations for the thorium molten salt reactor and advantages of the fast non-moderated version. Nucl. Sci. Eng. 161, 78–89.

Merle-Lucotte, E., Heuer, D., 2012. Preliminary design assessment of the molten salt fast reactor. In: Proceedings European Nuclear Conference ENC2012, Manchester, UK.

Merle-Lucotte, E., Heuer, D., Allibert, M., Brovchenko, M., Ghetta, V., Rubiolo, P., Laureau, A., 2013. Recommandations for a demonstrator of molten salt fast reactor. In: Proceedings of the International Conference on Fast Reactors and Related Fuel Cycles: Safe Technologies and Sustainable Scenarios (FR13), Paris, France.

Nuttin, A., et al., 2005. Potential of thorium molten salt reactors: detailed calculations and concept evolution with a view to large scale energy production. Prog. Nucl. Energy 46, 77–99.

Rineiski, A., 2008. Decay heat production in a TRU burner. Prog. Nucl. Energy 50, 377–381.

Rouch, H., Geoffroy, O., Rubiolo, P., Laureau, A., Brovchenko, M., Heuer, D., Merle-Lucotte, E., 2014. Preliminary thermal–hydraulic core design of the Molten Salt Fast Reactor (MSFR). Ann. Nucl. Energy 64, 449–456.

Serp, J., 2014. The molten salt reactor (MSR) in generation IV: Overview and perspectives. Prog. Nucl. Energy 77, 308–319.

Wang, S., Rineiski, A., Maschek, W., 2006. Molten Salt related extensions of the SIMMER-III code and its application for a burner reactor. Nucl. Eng. Des. 236, 1580–1588.

Wang, S., Rineiski, A., Zhang, D., 2013. Molten salt fast reactor analyses with SIMMER-III. In: Proceedings of American Nuclear Society 2013 Annual Meeting, Atlanta, USA.

Wang, S., Rineiski, A., Li, R., Brovchenko, M., Merle-Lucotte, E., Heuer, D., Laureau, A., Rouch, H., Aufiero, M., Cammi, A., Fiorina, C., Guerrieri, C., Losa, M., Luzzi, L., Ricotti, M.E., Kloosterman, J.-L., Lathouwers, D., van der Linden, E., Merk, B., Rohde, U., et al., 2014. Safety analysis – transient calculations of the MSFR – EVOL project. Deliverable 2, 6.

Weinberg, A.M., 1970. Collection of papers on the molten salt reactor experiment. Nucl. Appl. Technol. 8.

Zhang, D., Rineiski, A., 2014. COUPLE, a time-dependent coupled neutronics and thermal-hydraulics code, and its applications to MSFR (ICONE22-30609). In: Proceedings of the 2014 22nd International Conference on Nuclear Engineering, ICONE22, Prague, Czech Republic.

Zhang, D., Rineiski, A., Qiu, S., 2009. Comparison of modeling options for delayed neutron precursor movement in a molten salt reactor. In: Proceedings of ANS Annual Meeting 2009, Atlanta, USA.

Zhang, D., Rineiski, A., Qiu, S., 2011. Kinetics models for safety studies of fluid-fuel reactors. In: Proceedings of ANS Annual Meeting 2011, Hollywood, USA.

Zhang, D., Zhai, Z.-G., Chen, X.-N, Wang, S., Rineiski, A., 2013. COUPLE, a coupled neutronics and thermal-hydraulics code for transient analyses of molten salt reactors. In: Proceedings of ANS Annual Meeting 2013, Atlanta, USA.